Hybrid pulmonary surfactant-coated nanogels mediate efficient *in vivo* delivery of siRNA to murine alveolar macrophages

Authors

Lynn De Backer[a,1], Thomas Naessens[b,1], Stefaan De Koker[b], Elisa Zagato[a], Jo Demeester[a], Johan Grooten[b,*], Stefaan C. De Smedt[a,*], and Koen Raemdonck[a].

[1] Both authors contributed equally to this work.

Affiliations

[a] Laboratory of General Biochemistry and Physical Pharmacy, Department of Pharmaceutics, Ghent University, Ottergemsesteenweg 460, Ghent, 9000, Belgium.

[b] Laboratory of Molecular Immunology, Department of Biomedical Molecular Biology, Ghent University, Technologiepark 927, Zwijnaarde, 9052, Belgium.

* Corresponding authors

Johan Grooten. Tel.: +3293313650; Fax: +3292217673

Stefaan C. De Smedt. Tel.: +3292648076; Fax: +3292648189

E-mail addresses authors:

lynn.debacker@ugent.be

Thomas.Naessens@astrazeneca.com

stefaan.dekoker@irc.ugent.be

elzagato.zagato@ugent.be

jo.demeester@ugent.be

Johan.Grooten@irc.ugent.be

stefaan.desmedt@ugent.be

koen.raemdonck@ugent.be

Abstract

The local delivery of small interfering RNA (siRNA) to the lungs may provide a therapeutic solution to a range of pulmonary disorders. Resident alveolar macrophages (rAM) in the bronchoalveolar lumen play a critical role in lung inflammatory responses and therefore constitute a particularly attractive target for siRNA therapeutics. However, achieving efficient gene silencing in the lung while avoiding pulmonary toxicity requires appropriate formulation of siRNA in functional nanocarriers. In this study, we evaluated pulmonary surfactant-coated dextran nanogels for the delivery of siRNA to rAM upon pharyngeal aspiration in BALB/c mice. Both the surfactant-coated and uncoated nanogels achieved high levels of siRNA uptake in rAM, yet only the surfactant-coated formulation could significantly reduce gene expression on the protein level. Surfactant-coated nanogels induced a profound downregulation of target mRNA levels, reaching 70% knockdown with ~1 mg kg^{-1} siRNA dose. In addition, only mild acute pro-inflammatory cytokine and chemokine responses were detected one day after nanoparticle aspiration, accompanied by a moderate neutrophil infiltration in the bronchoalveolar lumen. The latter could be substantially reduced by removal of excess surfactant from the formulation. Overall, our hybrid core-shell nanoparticles have demonstrated safe and effective siRNA delivery to rAM, providing a new therapeutic approach for treatment of inflammatory pathologies in the lung.

Keywords

Dextran nanogel; *in vivo* test; macrophage; pulmonary surfactant; pulmonary delivery; siRNA

1. Introduction

Activation of the RNA interference (RNAi) pathway by synthetic RNA duplexes, termed small interfering RNAs (siRNAs), enables highly efficient and sequence-specific gene silencing. The application of siRNAs, designed to block the expression of disease-related proteins, has therefore emerged as a promising therapeutic strategy for the treatment of various diseases [1-3].

Pulmonary disorders, including chronic obstructive pulmonary disease (COPD) and lower respiratory infections, are currently amongst the top ten causes of death worldwide [4, 5]. Many of these diseases are characterized by an underlying inflammation. Phagocytic cells, *in casu* resident alveolar macrophages (rAM), significantly contribute to this inflammatory phenotype [6, 7] and thus are attractive targets for genetic interference.

Inhalation therapy provides a non-invasive way to locally deliver high amounts of siRNA directly to pulmonary target cells. However, the respiratory tract imposes substantial barriers that need to be overcome to allow effective siRNA delivery in the target cell cytoplasm [8]. For instance, the cell membrane is impermeable for hydrophilic macromolecules like nucleic acids, precluding direct access of siRNA to the intracellular RNAi machinery. Moreover, it has been reported that free siRNA is more rapidly distributed to the systemic circulation upon local pulmonary application, which decreases the siRNA dose in the bronchoalveolar lumen [9]. To avoid systemic exposure and enhance cellular delivery of siRNA to target cells, siRNAs typically require formulation into lipid- or polymer-based drug carriers. Although it was previously assumed that nanoparticles are able to bypass the phagocytic uptake by rAM [10], recent findings illustrated that rAM preferably capture particles with a hydrodynamic diameter in the nanometer scale [11-13]. A multitude of novel siRNA nanocarriers has already been tested *in vitro*. Still, to date only a limited number of nanoparticles have been evaluated for local *in vivo* siRNA delivery to rAM, with variable success [14-16].

Earlier work by our group demonstrated that cationic biodegradable dextran nanogels (NGs) are promising siRNA nanocarriers *in vitro*. They are able to encapsulate high amounts of siRNA and induce a marked gene knockdown in distinct cultured cell types [17-19]. Moreover, their stability and biodistribution has already been evaluated upon systemic application *in vivo* [20, 21]. Recently, a method has been optimized by us to combine the siRNA-loaded NGs (siNGs) with a clinically-approved pulmonary surfactant (Curosurf®) in a single core-shell nanoparticle, consisting of a siNG core layered with a pulmonary surfactant outer shell. The presence of the Curosurf® shell provided several beneficial traits, including improved stability and a five-fold enhancement of intracellular siRNA delivery in cultured lung cancer cells [22]. Given the significance of rAM as a target cell in many lung-related pathologies and the impressive siRNA delivery capacity of this hybrid core-shell nanoparticle, the key objective of this study was to evaluate if pulmonary surfactant-coated siNGs are equally efficient in transfecting murine rAM *in vivo* following pulmonary delivery.

The biological efficacy of the siNGs, in the absence or presence of a pulmonary surfactant shell, was first investigated in a murine alveolar macrophage cell line (MH-S), using the pan-leucocyte marker *cd45* as model target gene. As the preparation of the hybrid nanoparticle requires an excess of pulmonary surfactant, which might influence cellular delivery and toxicity, we additionally sought to optimize a purification protocol for our formulation. To probe their suitability for *in vivo* siRNA delivery, BALB/c mice were treated with the distinct nanoparticles *via* pharyngeal aspiration. The cellular internalization of the (pulmonary surfactant-coated) siNGs and subsequent CD45 knockdown was quantified in primary rAM recovered from bronchoalveolar lavage (BAL) as a function of time following *in vivo* pulmonary administration. Next to efficient delivery, it is of equal importance to design delivery systems with an acceptable safety profile. To determine the acute local inflammatory response,

we quantified the expression levels of various cytokines and chemokines in the bronchoalveolar lumen and assessed the infiltration of inflammatory cells, one day following pharyngeal aspiration.

2. Materials and Methods

2.1. Small interfering RNAs

Twenty-one nucleotide siRNA duplexes targeted against the protein tyrosine phosphatase receptor type C (CD45), hereafter abbreviated as siCD45, and non-targeting negative control duplexes (siCTRL) were purchased from Eurogentec (Seraing, Belgium). Both sense and antisense strands had a UU-overhang at the 3'-end and 5'-ends of antisense strands were phosphorylated. SiCD45: sense strand = 5'-GAA-GAA-UGC-UCA-CAG-AUA-A-3'; antisense strand = 5'-UUA-UCU-GUG-AGC-AUU-CUU-C-3'. SiCTRL: sense strand = 5´-UGC-GCU-ACG-AUC-GAC-GAU-G-3´; antisense strand = 5´-CAU-CGU-CGA-UCG-UAG-CGC-A-3´. For fluorescence experiments, the siCTRL duplex was labeled with a Cy5 dye at the 5' end of the sense strand (siCy5). The fluorescent modifications were performed and verified by Eurogentec. The concentration of the siRNA stock solutions in nuclease-free water (Ambion®-Life Technologies, Ghent, Belgium) was calculated from absorption measurements at 260 nm (1 $0D_{260}$ = 40 µg mL^{-1}) with a Nanodrop 2000 spectrophotometer (Thermo Fisher Scientific, Rockford, USA).

2.2. Synthesis of dextran nanogels and loading with siRNA

Cationic dextran nanogels were prepared using an inverse mini-emulsion photopolymerization method as reported previously [17]. Dextran hydroxyethyl methacrylate (dex-HEMA) with a degree of substitution of 5.2 [23] was selected for the preparation of the dextran nanogels based on previous work [24].

Briefly, 150 mg of dex-HEMA was dissolved in a solution containing 97.5 µL irgacure 2959 (10 mg mL^{-1} in water; Sigma-Aldrich, Bornem, Belgium), 180 µL nuclease-free water and 195 µL of a cationic methacrylate monomer, [2-(methacryloyloxy)-ethyl] trimethylammonium chloride (TMAEMA, 80 wt% solution in water; Sigma-Aldrich). The obtained dex-HEMA solution was emulsified in 5 mL of mineral oil (Sigma-Aldrich), supplemented with the surfactant ABIL EM 90 (0.5 mL) (Evonik Goldschmidt GmbH, Essen, Germany), through ultrasonication (90 s, amplitude 15 %; Branson Digital Sonifier®, Danbury, USA). The formed emulsion nanodroplets were immediately cross-linked by UV irradiation (900 s, Bluepoint 2.1 UV source, Hönle UV technology, Gräfelfing, Germany) under cooling (4°C). The resulting dex-HEMA-*co*-TMAEMA nanogels, hereafter abbreviated as NGs, were collected by precipitation in acetone and washed four times with acetone:hexane (1:1). Traces of organic solvent were removed by vacuum evaporation and the pellet was redispersed in 5 mL nuclease-free water. To assure long-term stability, the NGs were lyophilized and stored desiccated.

Prior to use, a NG stock (10 mg mL^{-1}) was prepared by dispersing a weighed amount of lyophilized particles in ice-cooled nuclease-free water, followed by short sonication (amplitude 10 %, Branson Digital Sonifier®). The NG stock contained less than 0.5 EU mL^{-1} lipopolysaccharide (LPS) as determined by the Endosafe®-PTS™ assay (Charles River International, Leco, Italy). To load NGs with siRNA, equal volumes of NG and siRNA dilutions in nuclease-free water were mixed and incubated at 4°C for ≥ 15 min to allow complexation.

2.3. Preparation of pulmonary surfactant-coated nanogels

A commercially available pulmonary surfactant, derived from minced porcine lungs (Curosurf®; Chiesi Pharmaceuticals, Parma, Italy), was used to construct the lipid coat. Pulmonary surfactant-coated siRNA-loaded NGs (siNGs) were prepared as described previously [22]. Briefly, Curosurf® was incubated with siNGs for 10 min at 4 °C, allowing electrostatic interaction. The ratio of surfactant-to-NGs equaled 10 mg Curosurf® (total phospholipids) per mg NGs. After incubation, the surfactant shell was formed by high-energy sonication, using a probe sonicator (amplitude 10 %).

2.4. Cryogenic transmission electron microscopy

Coated NGs were formed according to the method described above. The ratio of surfactant to NGs equaled 7.5 mg Curosurf® per mg NGs. 2.5 µL of the different samples was placed on a glow discharged holey carbon coated grid (Quantifoil® R 3.5/1, Quantifoil Micro Tools GmbH, Grosslöbichau, Germany). The excess of liquid was blotted with a filter paper, reducing the droplet to a thin film. The samples were vitrified in liquid ethane, using a vitrobot (FEI, Eindhoven, The Netherlands) and stored in liquid nitrogen until observation. The grids were transferred to a cryo specimen holder type 626 (Gatan GmbH, München, Germany) and observed in a CM 120 cryo-electron microscope (Philips, Eindhoven, The Netherlands) operating at 120 keV. Images were recorded on a slow-scan CCD camera (Gatan GmbH) under low-dose conditions.

2.5. Purification of the pulmonary surfactant-coated nanogels

The surfactant-coated siNGs were separated from excess surfactant by centrifugation through a 7.5 wt% OptiPrep™ (Sigma-Aldrich) cushion for 30 min at 30000 g (L8-70M Centrifuge with SW55 Ti rotor; Beckman Coulter, Suarlée, Belgium). The supernatant, enclosing empty surfactant vesicles, was removed. The resulting pellet, containing the purified surfactant-coated NGs (abbreviated as coated NGs-P), was resuspended in nuclease-free water. Subsequently, equal volumes of the resuspended formulation and double-concentrated phosphate buffered saline (PBS; Gibco®-Life Technologies) were mixed, in order to obtain physiological salt concentrations.

2.6. Nanoparticle concentration determined by fluorescence single particle tracking

Fluorescence single particle tracking (fSPT) is a technique that monitors the diffusional movement of individual fluorescently labeled nanoparticles using a highly sensitive fluorescence microscope setup as described in [25]. Besides the size of nanoparticles, this technique also allows to accurately measure the absolute number concentrations of nanoparticles dispersed in complex biological fluids [26]. In our experiments, a swept-field confocal microscope (Eclipse Ti; Nikon, Brussels, Belgium) with a solid-state 125 mW 640 nm and 20 mW 488 nm laser (Agilent Technologies, Santa Clara, USA) laser was used to excite the fluorophores in samples mounted on the microscope equipped with a Plan Apo VC 100x 1.4 NA oil immersion objective lens (Nikon). A fast and sensitive EMCCD camera (Ixon Ultra 897; Andor Technology, South Windsor, USA) recorded high-speed movies of the individual particles diffusing in the dispersion. Particle trajectories were subsequently calculated using in-house developed software [25].

In this work, the technique was used to simultaneously determine the concentration of fluorescently-labeled siNGs and empty pulmonary surfactant present in the surfactant-coated siNG dispersion, before and after purification. Prior to use for siNG coating, Curosurf® was mixed with 2.5 wt% (of the total phospholipids) lipid-like dye DIO (Invitrogen™ – Life Technologies) in chloroform:methanol (2:1). A lipid film was formed by rotary evaporation of the organic solvents under vacuum at 37 °C. The dried lipid film was rehydrated in nuclease-

free water under mechanical agitation. The NGs were loaded with Cy5-labeled siRNA (10 pmol per µg NG). A total of 5 µL of the thus obtained dual-labeled surfactant-coated siNGs was then applied between a microscope slide and a cover glass with a double-sided adhesive sticker of 120 µm thickness in between (Secure-Seal Spacer, Molecular Probes, Leiden, The Netherlands). The microscope was always focused at ± 20 µm above the cover glass to avoid deviations from free diffusion. For each sample, 25 movies of approximately 200 frames each were recorded at different locations within the sample.

2.7. Cell line and culture conditions

All cell culture experiments in this study were conducted on murine alveolar macrophages (MH-S). The cells were grown in RPMI 1640 medium, supplemented with 2 mM glutamine, 10 % fetal bovine serum (FBS), 100 U mL^{-1} penicillin/streptomycin, 0.05 mM 2-mercaptoethanol, 0.01 M N-2-hydroxyethylpiperazine-N'-2-ethanesulfonic acid (HEPES), and 1 mM sodium pyruvate. All materials were purchased from Gibco®-Life Technologies, except for the serum, which was delivered by Hyclone™ (Thermo Fisher Scientific). The cells were cultured at 37 °C in a humidified atmosphere containing 5 % CO_2. Cells were passed every 3 days using 0.25 % trypsin/ethylenediamine-tetraacetic acid (EDTA) solution (Gibco®-Life Technologies) in order to maintain subconfluency.

2.8. In vitro quantification of cellular internalization and gene silencing by flow cytometry

Twenty-four hours before transfection, MH-S cells were seeded in 12-well plates (Greiner Bio-One GmbH, Frickenhausen, Germany) at a density of $4x10^4$ cells per cm^2.

To quantify the cellular internalization, NGs were loaded with different amounts of siRNA, labeled with 0.75 mol% Cy5. After five-fold dilution in Opti-MEM® (Gibco®-Life Technologies), resulting in a final NG concentration of 20 µg mL^{-1} and a final siRNA concentration of 100 nM, 10 nM or 1 nM, the samples were brought onto the cells. Following incubation (4 h), the cells were washed with PBS and incubated with dextran sulfate sodium salt (0.1 mg mL^{-1} in PBS) to remove surface bound fluorescence. Next, the cells were harvested by trypsinization (trypsin/EDTA 0.25 %) whose activity was halted by adding complete cell culture medium. Following centrifugation (7 min, 300 g), the cell pellet was resuspended in 250 µL flow buffer (PBS supplemented with 1 % bovine serum albumin and 0.1 % sodium azide) and placed on ice until flow cytometric analysis.

To determine the silencing potential of the different formulations, NGs were loaded with varying amounts of siCD45. The CD45 expression was normalized to that of cells treated with a negative control siRNA sequence (siCTRL). Upon 4 h of incubation, the cells were washed with PBS and 1 mL of culture medium was added. Two days post-transfection, the cells were detached with a non-enzymatic cell dissociation buffer (10 min incubation at 37°C). After centrifugation (7 min, 300 g), the cell pellet was resuspended in staining buffer (PBS supplemented with 5 % FBS). High-affinity Fc receptors were blocked by incubation with purified anti-mouse CD16/CD32 (BD Biosciences, Erembodegem, Belgium) for 15 min at 4 °C. Subsequently, the cells were incubated with PerCP-Cy™ 5.5 rat antimouse CD45 (BD Biosciences) diluted in staining buffer for 45 min at room temperature. Following three washing steps with 1 mL staining buffer, the cell pellet was resuspended in 250 µL flow buffer and placed on ice until flow cytometric analysis.

A minimum of 10^4 cells was analyzed in each measurement, using a FACSCalibur™ flow cytometer (BD Biosciences). The fluorescence detector for Cy5-labeled siRNA and for PerCP-Cy™ 5.5 labeled antibody detects wavelengths of 661 nm (± 16 nm) and above 670 nm, respectively. Data analysis was performed using the CellQuest Pro™ analysis software (BD Biosciences).

2.9. Mice

Female BALB/c mice were purchased from Charles River International and housed on a 12 h light/dark schedule. All mice were 6 to 8 weeks old at the start of the experiments. All procedures involving animals were approved by the local Ghent University ethics committee. Mouse pharyngeal aspiration was used for pulmonary administration. Briefly, after anesthetization *via* an intraperitoneal injection of a ketamine/xylazine mixture, the mouse was placed in a near-vertical position. The animal's tongue was extended with lined forceps, and 80 µL of the nanoparticle dispersion was placed posterior of the pharynx. The tongue was held in position until the dispersion was inhaled into the lungs. Control mice were administered 80 µL of PBS.

2.10. Bronchoalveolar lavage

At different time intervals upon aspiration, mice were sacrificed by intraperitoneal application of a lethal dose of Nembutal® (200 mg kg^{-1}; Ceva, Brussels, Belgium). A lavage cannula was immediately placed into the trachea through a small incision. The lungs were flushed four times with 1 mL Ca^{2+}- and Mg^{2+}- free Hank's balanced salt solution (HBSS; Invitrogen™-Life Technologies), supplemented with 0.05 mM EDTA. The obtained bronchoalveolar lavage (BAL) was subsequently centrifuged, to separate the cellular fraction present in the lavage from the BAL fluid (BALF).

2.11. Assessment of acute in vivo toxicity

Dose-dependent acute local inflammatory responses were evaluated for NGs, surfactant-coated NGs, and purified surfactant-coated NGs (coated NGs-P). Importantly, in these experiments the mice were treated with unloaded nanoparticles, in order to exclude the influence of siRNA on the innate immune system and thus to assess the acute inflammatory features of the nanoparticles as such. Doses were adjusted by altering the concentration of the particles (i.e. 1.25 mg mL^{-1}; 2.5 mg mL^{-1}, 3.75 mg mL^{-1}). The aspirated volumes were held constant at 80 µL. Additionally, mice were treated with Curosurf® vesicles, at the highest dose present in the most concentrated surfactant-coated NG formulation (i.e. 3000 µg phospholipids). As a negative control, mice were treated with PBS. One day after aspiration, the BAL samples were isolated from the treated mice. Both the cytokine and chemokine expression levels in the BALF, and the cellular infiltration in the BAL, were determined.

Protein levels of mouse TNF-α, IL-1α, IL-6, CXCL1, and MCP-1 in BALF were quantified with a Bioplex Suspension array system (Biorad, Hercules, USA) according to manufacturer's specifications. The analytes were measured with a Luminex protein array reader and Bio-Plex manager software version 5.0 (Bio-Rad Laboratories), using recombinant standards (Bio-Rad Laboratories). For data analysis, a 5-parameter logistic curve fit was applied to each standard curve and sample.

The total number of BAL cells was counted, after lysis of RBCs with ammonium potassium chloride lysis buffer, by use of a Bürker chamber (Brand GmbH, Wertheim, Germany). Trypan blue was added to exclude dead cells. The differential BAL cell counts were analyzed by flow cytometry. Cells, pre-incubated with Fc Block (purified anti-mouse CD16/CD32; BD Biosciences), were classified as monocytes, eosinophils, neutrophils, or lymphocytes based on forward and side scatter pattern and fluorescence intensities of anti-mouse CD3-Alexa488, SiglecF-PE, CD4-PerCP (all from BD Biosciences), CD11c-PE-TR (Invitrogen™, Life Technologies) MHCII-v450, CD8-PE-Cy7 and CD11b-APC-eFluor780 (all from eBioscience; Vienna, Austria). Sytox Red (Molecular Probes®, Life Technologies) staining was performed to exclude dead cells.

2.12. Uptake in resident alveolar macrophages

The ability of resident alveolar macrophages (rAM) to internalize NGs loaded with fluorescently-labeled siRNA (siCy5) was assessed by flow cytometry. Briefly, siCy5 was complexed with the lowest NG dose in previous experiment (100 µg) at a ratio of 1 pmol siCy5 per µg NGs. Mice were treated with free siRNA, siNGs, surfactant-coated siNGs or surfactant-coated siNGs-P (*n*=4). At various time points after treatment, BAL was collected as described above. First, high-affinity Fc receptors were blocked by incubation with purified anti-mouse CD16/CD32 (BD Biosciences) for 15 minutes at 4°C. Next, the rAM were selected based on their forward and side scatter pattern, intrinsic autofluorescence and their surface marker profile, using an antibody against CD11c (CD11c-PE-TR), SiglecF (SiglecF-PE) and Ly6C (Ly6C-v450; BD Biosciences). The samples were measured on a FACSLSRII™ flow cytometer (BD Biosciences). Data analysis was performed using the FlowJo™ analysis software (Treestar, Costa Mesa, USA).

2.13. Silencing in resident alveolar macrophages

The *in vivo* silencing potential of the different formulations in rAM was assessed on protein level, using flow cytometry, and on RNA level, using real-time quantitative PCR (qPCR). Here, mice were treated with 22.5 µg active siRNA, designed to selectively reduce CD45 expression (siCD45), or 22.5 µg negative control siRNA (siCTRL).

To determine the gene expression on protein level, mice were treated with the same samples as described above (*n*=4, NG dose of 100 µg). BAL was collected after 24 h, 48 h, or 96 h and the CD45 expression profile in rAM was determined by fluorescently-labeled CD45 antibody (PerCP-Cy™ 5.5 rat antimouse CD45; BD Biosciences).

To evaluate the transcriptional level of the *cd45* gene by qPCR, mice were treated with surfactant-coated siNGs (final NG dose = 100 µg). As a negative control, mice were treated with PBS. One day after the aspiration, the mice were sacrificed and the BAL was isolated. The alveolar macrophages were collected from BAL by the magnetic-activated cell sorter separation system using anti-CD11c microbeads (Miltenyi Biotec, Auburn, USA). RNA isolation from the alveolar macrophages was completed using an RNeasy Plus mini kit (Qiagen, Hilden, Germany) according to manufacturer's protocol. cDNA was synthesized using a iScript™ cDNA synthesis kit (Bio-Rad Laboratories). Real-time quantitative PCR (qPCR) was performed on a LightCycler 480 system using a qPCR kit for SYBR Green I (Roche Molecular Systems, Pleasanton, USA). Real-time qPCR amplification was performed in triplicate reactions under the following conditions: a pre-incubation step at 95°C for 5 min, followed by 50 cycles at 95°C for 10 s and at 60°C for 30 s. The following primers were used: *Murine cd45_1* forward primer = 5'-CAGAAACGCCTAAGCCTAGTTG-3'; reverse primer = 5'-AGGCAAGTAGGGACACTTCATAG-3'. *Murine cd45_2* forward primer = 5'-ATAT CGCGGTGTAAAACTCGTC-3'; reverse primer = 5'-TAGGCTTAGGCGTTTCTGGAA-3'. *Murine rpl13a* forward primer = 5'=-CCTGCTGCTCTCAAGGTTGTT-3'; reverse primer = 5'-TGGCTGTCACTGCCTGGTACTT-3'. *Murine tbp* forward primer = 5'- TCTACCGTG AATCTTGGCTGT AAA-3'; reverse primer = 5'-TTCTCATGATGACTGCAGCAAA-3'. *Murine b2m forward primer = 5'*-ATGCACGCAGAAAGAAATAGCAA-3'; reverse primer = 5'-AGCTATCTAGGATATTTCCAATTTTTGAA-3'. *Murine rpl13a*, *tbp and b2m* mRNA was used as reference housekeeping gene for normalization [27]. All primers were purchased from Invitrogen™ (Life Technologies). The relative mRNA expression is presented by means of n-fold induction when compared with PBS-treated mice.

2.14. Statistical analysis

All data are presented as mean ± standard error (SEM). Presented data are representative for at least 2 independent experiments. Statistical analyses were performed by one- and two-way

ANOVA with Bonferroni correction, using GraphPad Prism software version 6. An unpaired t-test was used to compare the transcriptional level of the *cd45* gene, as determined by qPCR.

3. Results

3.1. Purification of the pulmonary surfactant-coated nanogels

We recently demonstrated that the cellular delivery capacity of siRNA-loaded nanogels (siNGs) could be significantly enhanced by decorating them with a pulmonary surfactant (Curosurf®) shell [22]. To this end, both cationic siNGs and anionic crude pulmonary surfactant are mixed to allow electrostatic interaction, followed by high-energy sonication to induce fusion of the pulmonary surfactant on the siNG surface [22]. Cryo-TEM imaging of the pulmonary surfactant-coated siNGs revealed two coexisting nanostructures: (i) the hybrid nanoparticles consisting of a siNG core layered with a unilamellar pulmonary surfactant shell and (ii) an excess of empty pulmonary surfactant vesicles (**Figure 1A**). It is conceivable that this surplus of Curosurf® could affect the cellular delivery of siRNA and the inflammatory response upon pulmonary administration. Therefore, we sought to optimize a procedure to separate the pulmonary surfactant-coated siNGs from empty pulmonary surfactant vesicles. As schematically depicted in **Figure 1B**, the protocol involves high-speed centrifugation through a 7.5 wt% OptiPrep™ cushion of which the selected density slightly exceeds that of the empty surfactant vesicles. As a result the latter vesicles remain on top of the cushion upon centrifugation, while the surfactant-coated siNGs are collected at the bottom.

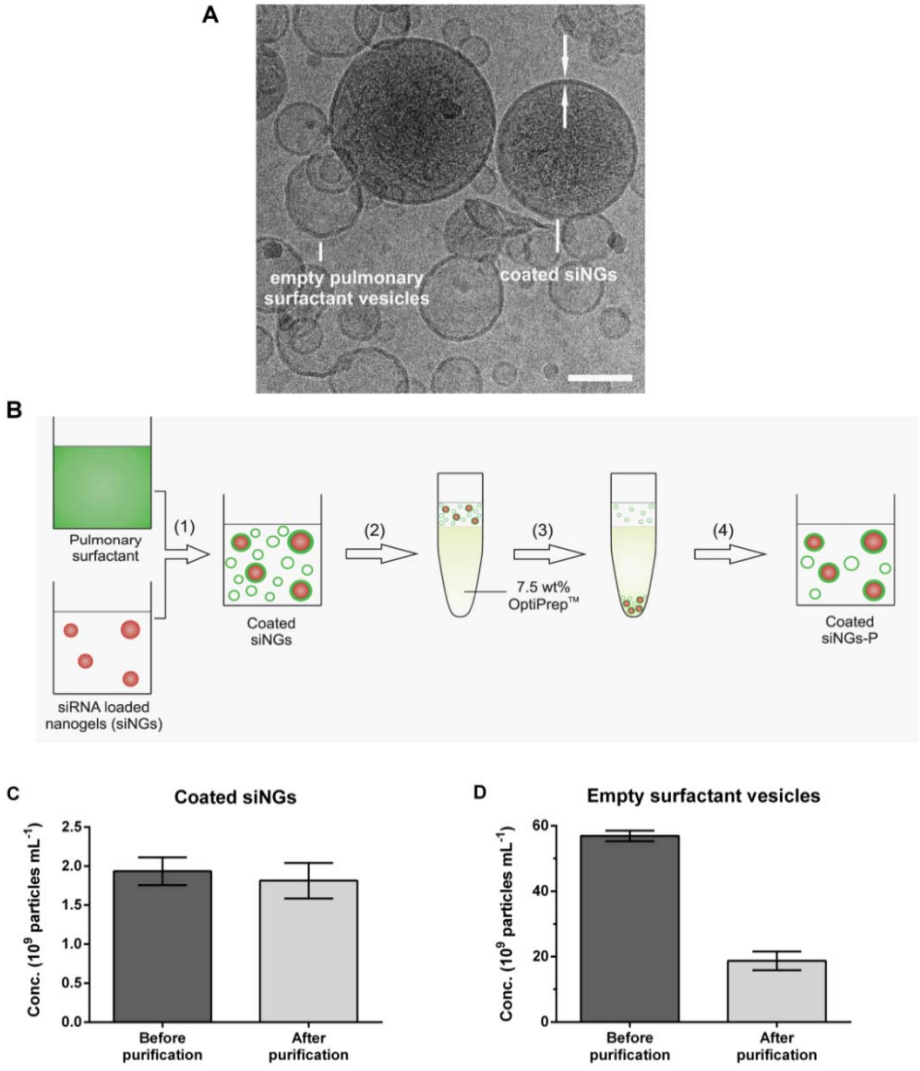

Figure 1. (A) Cryogenic transmission electron microscopy images of the pulmonary surfactant-coated siRNA-loaded nanogels (coated siNGs). The white arrows mark the pulmonary surfactant coat. The scale bar corresponds with 100 nm. **(B)** Scheme illustrating the different steps involved in the separation of the coated siNGs from the empty pulmonary surfactant vesicles. (1) The pre-formed siNGs interact with the unprocessed surfactant dispersion. Hereafter, phospholipid fusion onto the nanogel surface is induced *via* probe sonication. (2) The coated siNG dispersion is layered on top of a 7.5 wt% OptiPrep™ cushion. (3) The tubes are centrifuged at 30000 g during 30 min (4 °C). (4) The supernatant is removed, including the empty pulmonary surfactant vesicles on top of the OptiPrep™ layer. The pellet is resuspended in nuclease-free water and mixed in equal volumes with double concentrated PBS, to obtain the purified coated siNGs (Coated siNGs-P). **(C and D)** Particle number concentration of the coated siNGs loaded with red fluorescent siRNA (10 pmol per μg NG) (C, *n*=5) and the empty Curosurf® vesicles labeled with the lipid-like dye DIO (2.5 wt%) (D, *n*=3), determined by dual-color fluorescence single particle tracking.

To assess the feasibility of this purification procedure, the concentration of both empty surfactant vesicles and surfactant-coated siNGs was determined before and after the centrifugation step, using fluorescence single particle tracking (fSPT). As described earlier, this technique allows accurate quantification of absolute number concentrations of fluorescently labeled nanoparticles in complex mixtures [25, 26]. To distinguish both particle types, Curosurf® was fluorescently labeled by insertion of the green fluorescent lipid-like dye DiO, while NGs were loaded with red fluorescent siRNA (siCy5). The dual-labeled nanoparticles were simultaneously illuminated by a 488 nm and 640 nm laser to allow quantification of both nanoparticle populations. We observed no significant loss of pulmonary surfactant-coated siNGs during the purification protocol (**Figure 1C**). Subtraction of the number of particles detected in the red channel (coated siNGs) from the number of particles detected in the green channel (coated siNGs and empty surfactant vesicles), yielded the concentration of the empty surfactant vesicles (**Figure 1D**). Importantly, it was shown that 67.2 % of the empty surfactant vesicles could be removed *via* this protocol.

3.2. In vitro siRNA delivery to alveolar macrophages

The capacity of the different nanoparticles to guide siRNA delivery to a murine alveolar macrophage cell line (MH-S) was evaluated. To this end, the cells were incubated with siNGs, surfactant-coated siNGs, or surfactant-coated siNGs after removal of free pulmonary surfactant vesicles (surfactant-coated siNGs-purified, abbreviated as coated siNGs-P). Free siRNA was included as a control and, as expected, no relevant internalization of free siCy5 by the cells could be detected (**Figure 2A**). Encapsulating the siRNAs in cationic siNGs markedly facilitated cellular uptake, in agreement with earlier reports on this formulation [17, 18]. The presence of a pulmonary surfactant outer shell significantly inhibited cellular uptake (**Figure 2A**), which was also observed earlier in cultured lung cancer cells [22]. This is most likely attributed to the shielding of the siNG positive charge with anionic pulmonary surfactant, thereby precluding efficient electrostatic interaction with the macrophage cell membrane.

In order to evaluate the *in vitro* gene silencing potential of the siRNA-loaded nanoparticles, protein tyrosine phosphatase receptor type C (CD45), which is expressed on the surface of all nucleated hematopoietic cell types, was selected as a model target. The data shown in **Figure 2B** demonstrate a significantly lowered expression level of CD45 protein, reaching 60 % knockdown for the uncoated siNGs at the highest siRNA dose. Note that the CD45 knockdown was only slightly reduced in the presence of the surfactant shell. Importantly, given the ten-fold reduction in intracellular siRNA dose upon coating, as shown in **Figure 2A**, it can be hypothesized that the pulmonary surfactant improves cytosolic siRNA delivery.

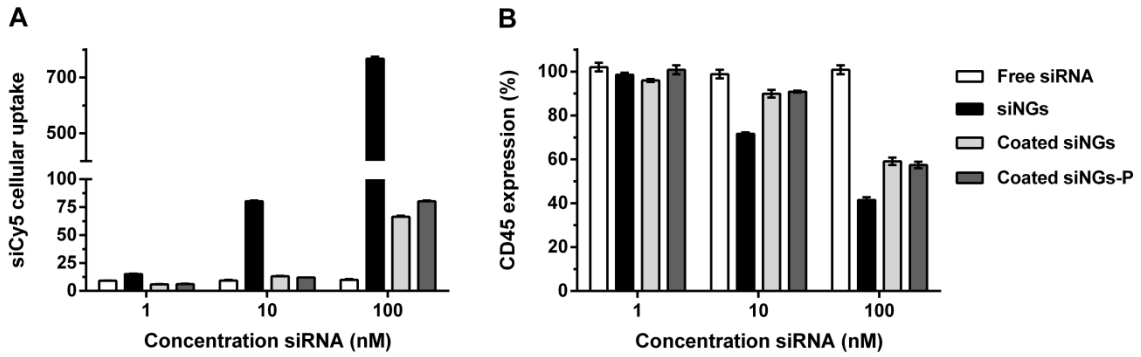

Figure 2. Cellular uptake and gene silencing potential of the different formulations in a murine alveolar macrophage cell line (MH-S), determined by flow cytometry. Evaluation of cellular uptake **(A)** and CD45 gene silencing potential **(B)** of free siRNA (white), siRNA complexed with nanogels (siNGs; black), pulmonary surfactant-coated siNGs (light gray) or purified pulmonary surfactant-coated siNGs (coated siNGs-P; dark gray), as a function of siRNA concentration. The experiments were performed with a fixed nanogel concentration (20 μg mL^{-1}). For the uptake experiments fluorescent siRNA was used (0.75 mol% Cy5-labeled). To determine the percentage CD45 expression, the CD45 expression of cells treated with active siRNA (siCD45) was normalized to that of cells treated with control siRNA (siCTRL). Data points represent geometric mean fluorescence intensities ± standard error (*n*=3).

3.3. Acute inflammatory effect in murine lungs

Since the pulmonary application of nanoparticles might induce an acute inflammatory response in the lungs [28], it is of particular importance to evaluate the *in vivo* pro-inflammatory effects of novel nanocarriers.

To this end, BALB/c mice were treated with increasing doses of the different aforementioned nanocarriers *via* pharyngeal aspiration. After 24 h, the bronchoalveolar lavage fluid (BALF) was collected and the levels of the pro-inflammatory cytokines IL-1α, IL-6 and TNF-α were quantified along with the levels of the chemokines CXCL-1 and MCP-1 (**Figure 3**).

In general, the aspiration of nanoparticles significantly enhanced the expression of all cytokines and chemokines in BALF, except for TNF-α, compared to the expression levels in placebo (PBS)-treated mice. Furthermore, the NGs elicited a dose-dependent response, showing elevated levels of most cytokines and chemokines at mounting NG doses (**Figure S1_A**). Importantly, this acute pro-inflammatory response could partially be reduced by shielding the NG surface with the pulmonary surfactant shell (**Figure S1_B**). Of note, aspiration of empty Curosurf® vesicles induced negligible secretion of inflammatory mediators. The latter observation likely also explains the comparable cytokine/chemokine expression levels for both coated NGs and coated NGs-P.

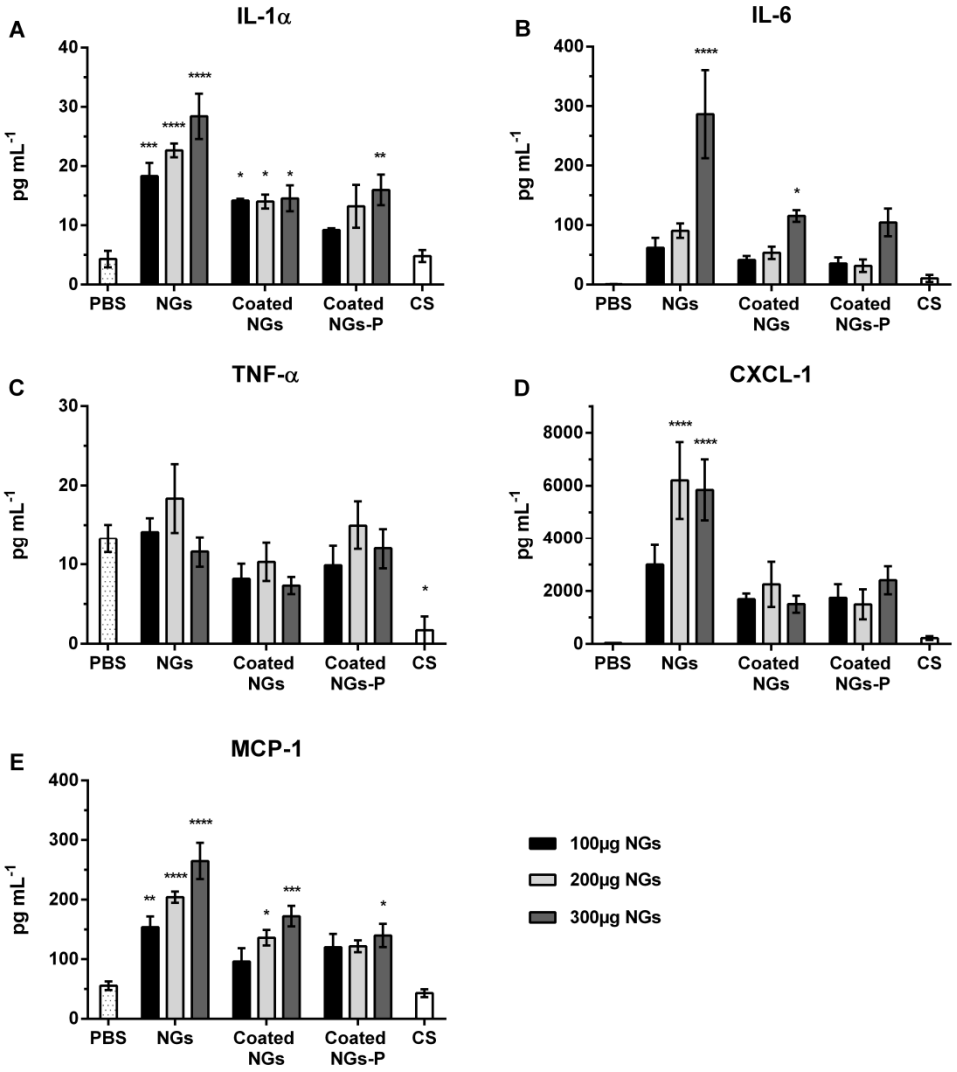

Figure 3. Cytokine (A-C) and chemokine (D,E) concentrations in bronchoalveolar lavage fluid of mice 24 h after treatment with nanogels (NGs), pulmonary surfactant-coated NGs or purified coated NGs (coated NGs-P). Mice were treated with increasing NG doses: 100 µg (black), 200 µg (light gray), or 300 µg (gray). Additionally, mice were treated with surfactant (Curosurf®) vesicles (CS). The aspirated dose equals the surfactant dose present in the most concentrated coated formulations (3000 µg of total phospholipids). As a negative control, mice were treated with PBS. The protein concentrations were measured using a Bio-Plex suspension array system, according to manufacturer's instructions. Data points represent average values ± standard error (n=4). The asterisks represent the statistical significance compared to PBS-treated mice (*$p \leq 0.05$, **$p \leq 0.01$, ***$p \leq$ 0.001, ****$p \leq 0.0001$).

Next, we evaluated the impact of the nanoparticles on the recruitment of inflammatory cells in the bronchoalveolar lavage (BAL). To this end, the total cell numbers in BAL 24 h after aspiration of increasing doses of nanoparticles were determined (**Figure 4A**). Contrarily to the elevated cytokine and chemokine levels, aspiration of NGs did not induce inflammatory cell infiltration even at the highest dose. However, coating of the NGs with surfactant elicited inflammatory cell recruitment at the highest dose of 300 µg NG. Likely, this inflammatory response resulted from the presence of free Curosurf® vesicles as indicated by the pronounced increment in bronchoalveolar inflammatory cell number observed following administration of Curosurf® vesicles alone and the lack of inflammatory cell recruitment when free surfactant vesicles were partially removed from the formulation (coated NGs-P).

In all instances, the dominant inflammatory cell type recruited to the alveolar compartment were neutrophils as illustrated in **Figure 4B**, showing the cell-type specific composition of the inflammatory cell infiltrate elicited by the lowest NG doses.

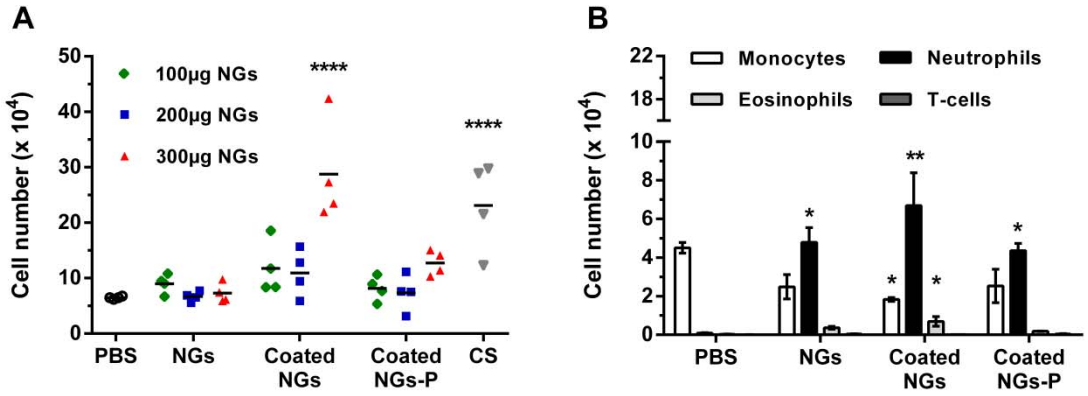

Figure 4. Cellular infiltration in the bronchoalveolar lavage (BAL) of mice treated with nanogels (NGs), pulmonary surfactant-coated NGs or purified coated NGs (coated NGs-P). As a negative control, mice were treated with PBS. **(A)** Total cell infiltration in BAL in response to the aspiration of increasing NG doses: 100 µg (green), 200 µg (blue), or 300 µg (red). The aspirated dose of Curosurf® vesicles (CS; gray) equals the dose present in the most concentrated coated formulations (3000 µg of total phospholipids). The individual data points and their corresponding average values were illustrated (n=4). **(B)** The differential cellular composition in BAL of mice treated with the different nanoparticles at the lowest NG dose (100 µg). Flow cytometric analysis differentiated monocytes (white), neutrophils (black), eosinophils (light gray), and T-cells (dark gray). Data points represent average values ± standard error (n=4). The asterisks represent the statistical significance compared to PBS-treated mice (*$p \leq 0.05$, **$p \leq 0.01$, ***$p \leq$ 0.001, ****$p \leq 0.0001$).

3.4. In vivo siRNA delivery to murine resident alveolar macrophages

Given the promising *in vitro* results, we sought to evaluate the potential of our formulations toward *in vivo* pulmonary siRNA delivery to resident alveolar macrophages (rAM). To evaluate this, the different nanoparticles, loaded with Cy5-labeled siRNA, were administered into the lungs of BALB/c mice *via* pharyngeal aspiration. The lowest NG doses (100 µg) were applied to minimize acute pulmonary inflammatory responses. BAL was collected at the indicated time points and analyzed by flow cytometry (**Figure 5**). rAM constitute the main phagocytic cell type in the bronchoalveolar lumen and were identified on the basis of their intrinsic high autofluorescence and the expression of the surface marker CD11c (**Figure 5A**). Already 4 h after treatment with siNGs and surfactant-coated siNGs, nearly all rAM had internalized Cy5-labeled siRNA. At 72 h, still 70% of the rAM population stained positive for Cy5-labeled siRNA upon aspiration of the surfactant-coated NGs, while a sharp drop to only 30% Cy5-positive rAM was observed after treatment with the uncoated siNGs (**Figure 5A**). Importantly, only a negligible percentage of Cy5-positive rAM were found in the lungs of mice treated with free siRNA.

Analysis of the Cy5 fluorescence intensities in rAM showed that, contrarily to the *in vitro* results, the surfactant shell did not cause an equivalent reduction in cellular internalization of siNGs *in vivo* (**Figure 5B).** Thus, in correspondence with the high percentages of Cy5-positive rAM at 4h and 24h, both siNGs and surfactant-coated siNGs yielded comparable levels of siCy5 uptake by the rAM. Strikingly, removal of excess free surfactant vesicles negatively impacted both the percentage of siCy5-positive rAM (**Figure 5A**) as the level of siCy5 uptake (**Figure 5B**). Yet, at the late 72h time-point, the differences between both coated formulations leveled off, both now showing an almost four-fold higher Cy5 fluorescence and a two-fold higher percentage of Cy5-positive rAM compared to rAM of mice treated with uncoated siNGs. This

result strongly points to an involvement of exogenous pulmonary surfactant in prolonging the residence time in the lung of the administered siRNA, hereby stabilizing or even increasing with time the levels of siCy5 uptake by rAM.

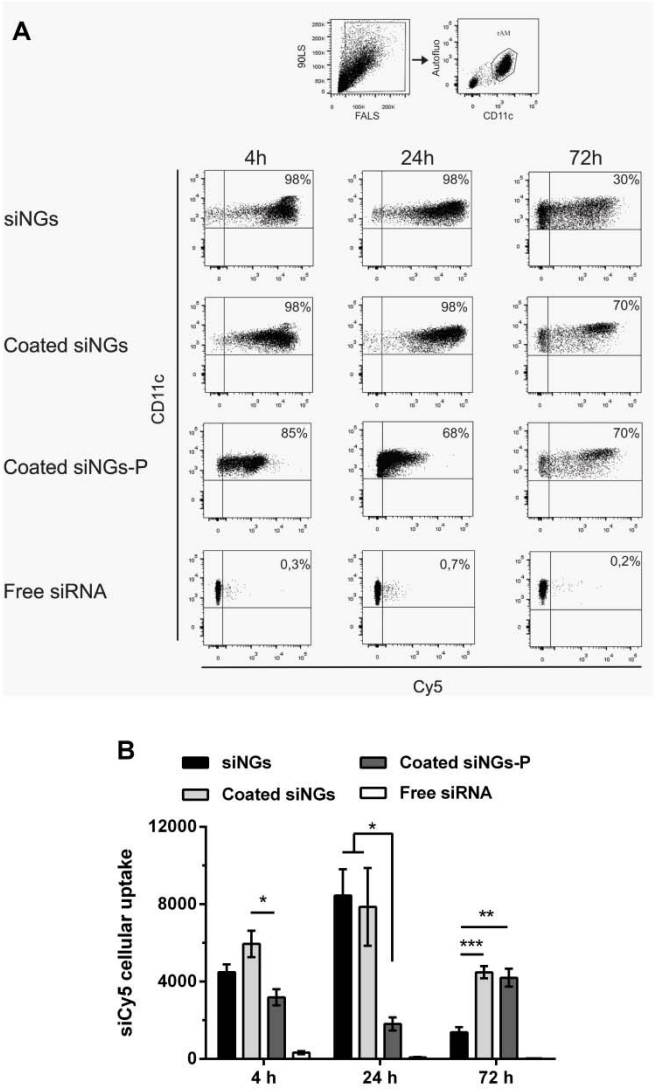

Figure 5. **Flow cytometric analysis of the uptake of fluorescent siRNA (siCy5) by resident alveolar macrophages (rAM) at different time points after aspiration. (A)** Dot plots of gated rAM indicate the percentage of Cy5-positive rAM in the bronchoalveolar lavage 4 h, 24 h, and 72 h after treatment with free siRNA or siRNA complexed with nanogels (siNGs), coated siNGs, or purified coated siNGs (coated siNGs-P). The respective percentages are depicted in each quadrant. **(B)** Geometric mean fluorescence intensities were quantified in rAM of mice treated with siNGs (black), coated siNGs (light gray), coated siNGs-P (dark gray), or free siRNA (white). Data represent average values ± standard error (n=4, *$p \leq 0.05$, **$p \leq 0.01$, ***$p \leq 0.001$).

3.5. In vivo gene silencing in resident alveolar macrophages

Having quantified the cellular internalization of Cy5-labeled siRNA, we next examined the efficiency of the different nanoparticle formulations to deliver functional siRNA, capable of mediating gene knockdown in rAM. Protein levels of the model target CD45 were analyzed by flow cytometry as a function of time following aspiration of the different nanoparticle formulations (**Figure 6**). Notably, the pulmonary delivery of negative control siRNA (siCTRL), either as free siRNA or complexed with the nanoparticles, resulted in elevated expression levels of CD45 protein by rAM 24 h and 48 h after treatment (**Figure 6A and 6B**). This effect even persisted for 96 h in mice treated with surfactant-coated siNGs and surfactant-coated siNGs-P (**Figure 6C**). This increased CD45 protein density on the surface of rAM is a known

phenomenon for hematopoietic cells, which control their CD45 phosphatase activity in response to different stimuli by altering CD45 protein levels [29]. Importantly, two days after treatment, only pulmonary delivery of surfactant-coated siNGs, loaded with active siCD45, resulted in a significant reduction of this CD45 upregulation, as compared to siCTRL (**Figure 6B**). At 96 h after treatment with surfactant-coated siNGs and surfactant-coated siNGs-P containing siCD45, CD45 expression levels decreased further to baseline levels (PBS), thus completely countering the treatment-induced increment in CD45 expression (**Figure 6C**).

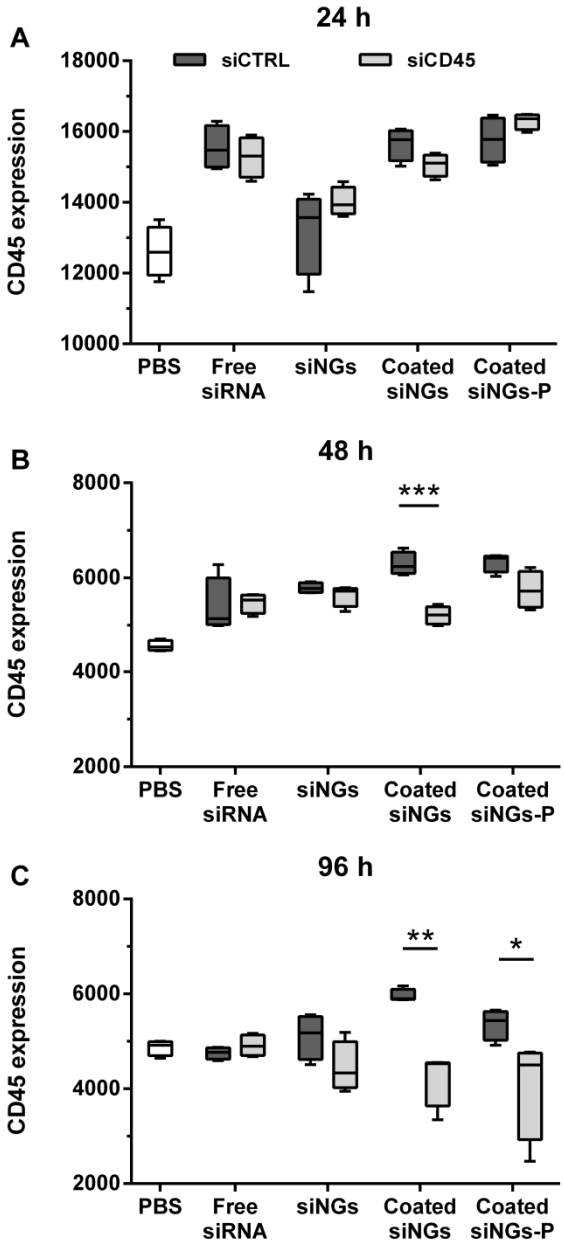

Figure 6. CD45 gene expression in resident alveolar macrophages (rAM) at different time points after treatment, determined by flow cytometry. Geometric mean fluorescence intensities of PerCP-Cy5.5-labeled CD45 antibodies were quantified in rAM of mice 24 h **(A)**, 48 h **(B)**, or 96 h **(C)** upon aspiration. The mice were treated with free siRNA, siRNA complexed with nanogels (siNGs), coated siNGs, or purified coated siNGs (coated siNGs-P). Both negative control siRNA sequences (siCTRL, dark gray), as active siRNA designed to selectively target CD45 (siCD45, light gray) were used. The data are represented in a box-and-whisker plot. The box extends from the 25th to 75th percentiles. The line in the middle of the box is plotted at the median. The whiskers go from the lowest to the highest value. (n=4; *$p \leq 0.05$, **$p \leq 0.01$, ***$p \leq 0.001$)

Since CD45 is a protein with a slow cell surface turnover, stable proteins residing at the plasma membrane could obscure the magnitude of the RNAi effect at the post-transcriptional level [29]. Therefore, we next aimed to determine CD45 silencing by quantifying *cd45* mRNA transcript levels in BAL-isolated rAM from treated mice. Given that our flow cytometric analysis already identified surfactant-coated siNGs as the most promising delivery system, we chose to focus only on this formulation. The transcriptional status of the *cd45* gene was evaluated by real-time quantitative polymerase chain reaction (RT-qPCR) one day after treatment. As shown in **Figure 7**, no elevated levels of *cd45* mRNA after treatment with surfactant-coated siNGs, loaded with siCTRL, could be detected in comparison to mRNA levels in PBS-treated mice. However, inhalation therapy with the surfactant-coated siNGs evoked an impressive and sequence-specific reduction in *cd45* mRNA, reaching up to 70 % knockdown.
Together, these results clearly show that pulmonary surfactant-coated siNGs successfully delivered active siRNA to rAM *in vivo*.

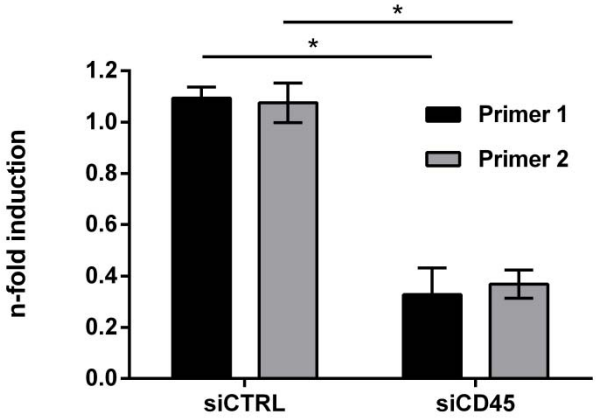

Figure 7. Transcriptional level of CD45 in resident alveolar macrophages of mice treated with coated siRNA-loaded nanogels (coated siNGs) 24 h after aspiration, determined by real-time quantitative polymerase chain reaction (qPCR) analysis. Results are given as the n-fold induction when compared with PBS-treated mice, for both CD45 primers used in the real-time qPCR amplification. The graph is a summary of two independent experiments. A minimum of 8 animals per group was necessary to achieve sufficient RNA concentrations. (*$p \leq 0.05$)

4. Discussion

Resident alveolar macrophages (rAM) are attractive targets for siRNA inhalation therapy due to their prominent role in multiple respiratory disorders, such as cystic fibrosis, asthma, tuberculosis, and chronic obstructive pulmonary disease [6, 7].
Following successful *in vitro* siRNA delivery to non-small cell lung cancer cells with pulmonary surfactant-coated siNGs [22], in this study we aimed to test the *in vivo* delivery potential of this core-shell nanoparticle to rAM in mice *via* pulmonary administration. Remarkably, we found a striking difference in the uptake of siRNA by rAM between *in vivo* and *in vitro* conditions. *In vitro*, internalization of cationic siNGs in a murine alveolar macrophage cell line (MH-S) was significantly suppressed by the presence of the anionic pulmonary surfactant shell, likely due to electrostatic repulsion by the negatively charged cell surface [18]. In contrast, following pharyngeal aspiration in BALB/c mice, both coated and uncoated siNGs were equally well internalized by rAM up to 24 h post-aspiration. This can possibly be attributed to the adsorption of negatively charged components from the endogenous alveolar surfactant onto the surface of the uncoated siNGs, as already illustrated in the literature for other types of nanoparticles [30, 31]. The *cd 45* gene was selected as a model target gene to

assess the RNAi effect [32]. Strikingly, despite the high intracellular siRNA doses in rAM obtained with both uncoated and surfactant-coated siNGs, only the latter were able to induce a significant CD45 knockdown in rAM. On the other hand, the removal of excess surfactant vesicles had a negative impact on the gene silencing potential, which could possibly be related to the significantly lower intracellular siRNA levels in rAM of mice treated with the purified formulation at the early time points (4 h and 24 h). Notably, the surfactant-coated siNGs were able to induce an effective siRNA-mediated gene knockdown, reaching 70 % knockdown in the difficult to transfect rAM, at a lower instilled siRNA dose compared to earlier work [14]. Together with our *in vitro* findings in MH-S cells, where a strong downregulation of CD45 expression was maintained despite the hampered cellular uptake, these results jointly hint toward a beneficial effect of the pulmonary surfactant on cellular siRNA delivery. However, the exact mechanism *via* which the pulmonary surfactant shell promotes delivery is not yet clear.

The benefit of a delivery vehicle for pulmonary administration of siRNA has been a subject of controversial discussion. In different pre-clinical models, a successful delivery in the respiratory tract of siRNA in the absence of a nanocarrier has been documented [33-35]. Moreover, promising results were obtained upon inhalation of free siRNA in human clinical trials for the treatment of patients infected with respiratory syncytial virus [36]. However, recent publications have clearly demonstrated the benefit of nanocarriers for siRNA inhalation therapy [9, 32, 37]. This was confirmed by our work, as the aspiration of free siRNA in the bronchoalveolar lumen of BALB/c mice resulted in negligible siRNA internalization by rAM and hence also failed to elicit a gene silencing effect. This observation underscores that in order to achieve delivery of siRNA to rAM, the siRNA should be formulated in an appropriate carrier, preferably in the nanometer range [11].

It is known from the literature that pulmonary administration of nanoparticles may trigger an acute local inflammatory response [28, 38]. Therefore, we assessed the levels of pro-inflammatory cytokines and chemokines in the bronchoalveolar lavage as well as the infiltration of inflammatory cells one day following pharyngeal aspiration of our nanoparticles, focusing on the role of the exogenous surfactant. Our results clearly revealed that excess of clinically approved pulmonary surfactant (Curosurf®) promoted a significant, yet conflicting impact on both the pro-inflammatory secretions and the cellular infiltrations.

Although it is conceivable that the expression levels of inflammatory mediators can change as a function of time [14], we clearly observed that the decoration of NGs with a pulmonary surfactant outer layer already significantly reduced the acute cytokine and chemokine responses evoked by bare cationic NGs. Moreover, comparable expression levels were observed for both surfactant-coated NGs and purified surfactant-coated NGs corroborating the negligible pro-inflammatory responses upon aspiration of empty Curosurf® vesicles, which is in agreement with earlier reports [39]. In contrast, cellular infiltration upon aspiration of surfactant-coated NGs at the highest NG dose was significantly increased compared to uncoated NGs, and the partial removal of excess surfactant from the formulation again alleviated this response. Also here, the latter can be correlated to the high cellular infiltrations detected upon the local application of empty Curosurf® vesicles, which is again in line with earlier observations [40].

5. Conclusions

Achieving safe and efficient gene silencing in the lung following pulmonary administration remains a challenging task. In this study, we identified pulmonary surfactant-coated dextran nanogels, consisting of a siRNA-loaded nanogel (siNG) core and a pulmonary surfactant (Curosurf®) outer shell, as a promising siRNA delivery system for this purpose. Pharyngeal aspiration of surfactant-coated siNGs provoked only a mild inflammatory cytokine response

and neutrophil infiltration in the bronchoalveolar lumen of BALB/c mice, but efficiently delivered siRNA to resident alveolar macrophages (rAM). The latter resulted in a substantial gene knockdown in rAM, which are notoriously difficult to transfect, with a relatively low siRNA dose (~1 mg kg^{-1}). Future research will be focused on evaluating biodistribution, toxicity and efficacy of this hybrid core-shell formulation for therapeutic siRNA delivery in validated disease models.

Acknowledgements

L. De Backer is a doctoral fellow of the Special Research Fund-Ghent University (BOF). K. Raemdonck and S. De Koker are postdoctoral fellows of the Research Foundation-Flanders, Belgium (FWO-Vlaanderen). T. Naessens is a postdoctoral fellow of the Special Research Fund-Ghent University (BOF12/GOA/014). Financial support of the Special Research Fund-Ghent University (BOF12/GOA/014) is also gratefully acknowledged.

References

[1] K. Raemdonck, R.E. Vandenbroucke, J. Demeester, N.N. Sanders, S.C. De Smedt, Maintaining the silence: reflections on long-term RNAi, Drug Discovery Today, 13 (2008) 917-931.
[2] B.L. Davidson, P.B. McCray, Jr., Current prospects for RNA interference-based therapies, Nat. Rev. Genet., 12 (2011) 329-340.
[3] R. Kole, A.R. Krainer, S. Altman, RNA therapeutics: beyond RNA interference and antisense oligonucleotides, Nat. Rev. Drug Discovery, 11 (2012) 125-140.
[4] C. Chang, Unmet Needs in Respiratory Diseases, Clin. Rev. Allergy Immunol., 45 (2013) 303-313.
[5] R. Lozano, M. Naghavi, K. Foreman, S. Lim, K. Shibuya, V. Aboyans, J. Abraham, T. Adair, R. Aggarwal, S.Y. Ahn, M. Alvarado, H.R. Anderson, L.M. Anderson, K.G. Andrews, C. Atkinson, L.M. Baddour, S. Barker-Collo, D.H. Bartels, M.L. Bell, E.J. Benjamin, D. Bennett, K. Bhalla, B. Bikbov, A. Bin Abdulhak, G. Birbeck, F. Blyth, I. Bolliger, S.A. Boufous, C. Bucello, M. Burch, P. Burney, J. Carapetis, H.L. Chen, D. Chou, S.S. Chugh, L.E. Coffeng, S.D. Colan, S. Colquhoun, K.E. Colson, J. Condon, M.D. Connor, L.T. Cooper, M. Corriere, M. Cortinovis, K.C. de Vaccaro, W. Couser, B.C. Cowie, M.H. Criqui, M. Cross, K.C. Dabhadkar, N. Dahodwala, D. De Leo, L. Degenhardt, A. Delossantos, J. Denenberg, D.C. Des Jarlais, S.D. Dharmaratne, E.R. Dorsey, T. Driscoll, H. Duber, B. Ebel, P.J. Erwin, P. Espindola, M. Ezzati, V. Feigin, A.D. Flaxman, M.H. Forouzanfar, F.G.R. Fowkes, R. Franklin, M. Fransen, M.K. Freeman, S.E. Gabriel, E. Gakidou, F. Gaspari, R.F. Gillum, D. Gonzalez-Medina, Y.A. Halasa, D. Haring, J.E. Harrison, R. Havmoeller, R.J. Hay, B. Hoen, P.J. Hotez, D. Hoy, K.H. Jacobsen, S.L. James, R. Jasrasaria, S. Jayaraman, N. Johns, G. Karthikeyan, N. Kassebaum, A. Keren, J.P. Khoo, L.M. Knowlton, O. Kobusingye, A. Koranteng, R. Krishnamurthi, M. Lipnick, S.E. Lipshultz, S.L. Ohno, J. Mabweijano, M.F. MacIntyre, L. Mallinger, L. March, G.B. Marks, R. Marks, A. Matsumori, R. Matzopoulos, B.M. Mayosi, J.H. McAnulty, M.M. McDermott, J. McGrath, G.A. Mensah, T.R. Merriman, C. Michaud, M. Miller, T.R. Miller, C. Mock, A.O. Mocumbi, A.A. Mokdad, A. Moran, K. Mulholland, M.N. Nair, L. Naldi, K.M.V. Narayan, K. Nasseri, P. Norman, M. O'Donnell, S.B. Omer, K. Ortblad, R. Osborne, D. Ozgediz, B. Pahari, J.D. Pandian, A.P. Rivero, R.P. Padilla, F. Perez-Ruiz, N. Perico, D. Phillips, K. Pierce, C.A. Pope, E. Porrini, F. Pourmalek, M. Raju, D. Ranganathan, J.T. Rehm, D.B. Rein, G. Remuzzi, F.P. Rivara, T. Roberts, F.R. De Leon, L.C. Rosenfeld, L. Rushton, R.L. Sacco, J.A. Salomon, U. Sampson, E. Sanman, D.C. Schwebel, M. Segui-Gomez, D.S. Shepard, D. Singh, J. Singleton, K. Sliwa, E. Smith, A. Steer, J.A. Taylor, B. Thomas, I.M. Tleyjeh, J.A. Towbin, T. Truelsen, E.A. Undurraga, N. Venketasubramanian, L. Vijayakumar, T. Vos, G.R. Wagner, M.R. Wang, W.Z. Wang, K. Watt, M.A. Weinstock, R. Weintraub, J.D. Wilkinson, A.D. Woolf, S. Wulf, P.H. Yeh, P. Yip, A. Zabetian, Z.J. Zheng, A.D. Lopez, C.J.L. Murray, Global and regional mortality from 235 causes of death for 20 age groups in 1990 and 2010: a systematic analysis for the Global Burden of Disease Study 2010, Lancet, 380 (2012) 2095-2128.
[6] L.C. Davies, S.J. Jenkins, J.E. Allen, P.R. Taylor, Tissue-resident macrophages, Nat. Rev. Immunol., 14 (2013) 986-995.

[7] T. Hussell, T.J. Bell, Alveolar macrophages: plasticity in a tissue-specific context, Nat. Rev. Immunol., 14 (2014) 81-93.
[8] O.M. Merkel, M. Zheng, H. Debus, T. Kissel, Pulmonary Gene Delivery Using Polymeric Nonviral Vectors, Bioconjug. Chem., 23 (2012) 3-20.
[9] S.A. Moschos, M. Frick, B. Taylor, P. Turnpenny, H. Graves, K.G. Spink, K. Brady, D. Lamb, D. Collins, T.D. Rockel, M. Weber, O. Lazari, L. Perez-Tosar, S.A. Fancy, C. Lapthorn, M.X. Green, S. Evans, M. Selby, G. Jones, L. Jones, S. Kearney, H. Mechiche, D. Gikunju, R. Subramanian, E. Uhlmann, M. Jurk, J. Vollmer, G. Ciaramella, M. Yeadon, Uptake, Efficacy, and Systemic Distribution of Naked, Inhaled Short Interfering RNA (siRNA) and Locked Nucleic Acid (LNA) Antisense, Mol. Ther., 19 (2011) 2163-2168.
[10] M. Geiser, W.G. Kreyling, Deposition and biokinetics of inhaled nanoparticles, Part. Fibre Toxicol., 7 (2010).
[11] F. Blank, P.A. Stumbles, E. Seydoux, P.G. Holt, A. Fink, B. Rothen-Rutishauser, D.H. Strickland, C. von Garnier, Size-Dependent Uptake of Particles by Pulmonary Antigen-Presenting Cell Populations and Trafficking to Regional Lymph Nodes, Am. J. Respir. Cell Mol. Biol., 49 (2013) 67-77.
[12] R.A. Roberts, T. Shen, I.C. Allen, W. Hasan, J.M. DeSimone, J.P.Y. Ting, Analysis of the Murine Immune Response to Pulmonary Delivery of Precisely Fabricated Nano- and Microscale Particles, PLoS One, 8 (2013).
[13] S. Takenaka, W. Moller, M. Semmler-Behnke, E. Karg, A. Wenk, O. Schmid, T. Stoeger, L. Jennen, M. Aichler, A. Walch, S. Pokhrel, L. Madler, O. Eickelberg, W.G. Kreyling, Efficient internalization and intracellular translocation of inhaled gold nanoparticles in rat alveolar macrophages, Nanomedicine (London, U.K.), 7 (2012) 855-865.
[14] A. Beyerle, A. Braun, O. Merkel, F. Koch, T. Kissel, T. Stoeger, Comparative in vivo study of poly(ethylene imine)/siRNA complexes for pulmonary delivery in mice, J. Controlled Release, 151 (2011) 51-56.
[15] S.A. Moschos, S.W. Jones, M.M. Perry, A.E. Williams, J.S. Erjefalt, J.J. Turner, P.J. Barnes, B.S. Sproat, M.J. Gait, M.A. Lindsay, Lung delivery studies using siRNA conjugated to TAT(48-60) and penetratin reveal peptide induced reduction in gene expression and induction of innate immunity, Bioconjug. Chem., 18 (2007) 1450-1459.
[16] U. Griesenbach, C. Kitson, S.E. Garcia, R. Farley, C. Singh, L. Somerton, H. Painter, R.L. Smith, D.R. Gill, S.C. Hyde, Y.H. Chow, J. Hu, M. Gray, M. Edbrooke, V. Ogilvie, G. MacGregor, R.K. Scheule, S.H. Cheng, N.J. Caplen, E.W.F.W. Alton, Inefficient cationic lipid-mediated siRNA and antisense oligonucleotide transfer to airway epithelial cells in vivo, Respir. Res., 7 (2006).
[17] K. Raemdonck, B. Naeye, K. Buyens, R.E. Vandenbroucke, A. Hogset, J. Demeester, S.C. De Smedt, Biodegradable Dextran Nanogels for RNA Interference: Focusing on Endosomal Escape and Intracellular siRNA Delivery, Adv. Funct. Mater., 19 (2009) 1406-1415.
[18] L. De Backer, K. Braeckmans, J. Demeester, S.C. De Smedt, K. Raemdonck, The influence of natural pulmonary surfactant on the efficacy of siRNA-loaded dextran nanogels, Nanomedicine (London, U.K.), 8 (2013) 1625-1638.
[19] L.B. Jensen, J. Griger, B. Naeye, A.K. Varkouhi, K. Raemdonck, R. Schiffelers, T. Lammers, G. Storm, S.C. de Smedt, B.S. Sproat, H.M. Nielsen, C. Foged, Comparison of Polymeric siRNA Nanocarriers in a Murine LPS-Activated Macrophage Cell Line: Gene Silencing, Toxicity and Off-Target Gene Expression, Pharm. Res., 29 (2012) 669-682.
[20] B. Naeye, H. Deschout, M. Roding, M. Rudemo, J. Delanghe, K. Devreese, J. Demeester, K. Braeckmans, S.C. De Smedt, K. Raemdonck, Hemocompatibility of siRNA loaded dextran nanogels, Biomaterials, 32 (2011) 9120-9127.
[21] B. Naeye, H. Deschout, V. Caveliers, B. Descamps, K. Braeckmans, C. Vanhove, J. Demeester, T. Lahoutte, S.C. De Smedt, K. Raemdonck, In vivo disassembly of IV administered siRNA matrix nanoparticles at the renal filtration barrier, Biomaterials, 34 (2013) 2350-2358.
[22] L. De Backer, K. Braeckmans, M.C. Stuart, J. Demeester, S.C. De Smedt, K. Raemdonck, Bio-inspired pulmonary surfactant-modified nanogels: A promising siRNA delivery system, J. Controlled Release, 206 (2015) 177-186.
[23] W.N.E. vanDijkWolthuis, S.K.Y. Tsang, J.J. KettenesvandenBosch, W.E. Hennink, A new class of polymerizable dextrans with hydrolyzable groups: hydroxyethyl methacrylated dextran with and without oligolactate spacer, Polymer, 38 (1997) 6235-6242.

[24] K. Raemdonck, B. Naeye, A. Hogset, J. Demeester, S.C. De Smedt, Prolonged gene silencing by combining siRNA nanogels and photochemical internalization, J. Controlled Release, 145 (2010) 281-288.
[25] K. Braeckmans, K. Buyens, W. Bouquet, C. Vervaet, P. Joye, F. De Vos, L. Plawinski, L. Doeuvre, E. Angles-Cano, N.N. Sanders, J. Demeester, S.C. De Smedt, Sizing Nanomatter in Biological Fluids by Fluorescence Single Particle Tracking, Nano Lett., 10 (2010) 4435-4442.
[26] M. Roding, H. Deschout, K. Braeckmans, M. Rudemo, Measuring absolute number concentrations of nanoparticles using single-particle tracking, Phys Rev E, 84 (2011).
[27] J. Vandesompele, K. De Preter, F. Pattyn, B. Poppe, N. Van Roy, A. De Paepe, F. Speleman, Accurate normalization of real-time quantitative RT-PCR data by geometric averaging of multiple internal control genes, Genome Biol., 3 (2002).
[28] R. Mohamud, S.D. Xiang, C. Selomulya, J.M. Rolland, R.E. O'Hehir, C.L. Hardy, M. Plebanski, The effects of engineered nanoparticles on pulmonary immune homeostasis, Drug Metab. Rev., 46 (2014) 176-190.
[29] M.L. Hermiston, Z. Xu, A. Weiss, CD45: A critical regulator of signaling thresholds in immune cells, Annu. Rev. Immunol., 21 (2003) 107-137.
[30] A.A. Kapralov, W.H. Feng, A.A. Amoscato, N. Yanamala, K. Balasubramanian, D.E. Winnica, E.R. Kisin, G.P. Kotchey, P.P. Gou, L.J. Sparvero, P. Ray, R.K. Mallampalli, J. Klein-Seetharaman, B. Fadeel, A. Star, A.A. Shvedova, V.E. Kagan, Adsorption of Surfactant Lipids by Single-Walled Carbon Nanotubes in Mouse Lung upon Pharyngeal Aspiration, ACS Nano, 6 (2012) 4147-4156.
[31] C.A. Ruge, U.F. Schaefer, J. Herrmann, J. Kirch, O. Canadas, M. Echaide, J. Perez-Gil, C. Casals, R. Muller, C.M. Lehr, The Interplay of Lung Surfactant Proteins and Lipids Assimilates the Macrophage Clearance of Nanoparticles, PLoS One, 7 (2012).
[32] A. Akinc, A. Zumbuehl, M. Goldberg, E.S. Leshchiner, V. Busini, N. Hossain, S.A. Bacallado, D.N. Nguyen, J. Fuller, R. Alvarez, A. Borodovsky, T. Borland, R. Constien, A. de Fougerolles, J.R. Dorkin, K.N. Jayaprakash, M. Jayaraman, M. John, V. Koteliansky, M. Manoharan, L. Nechev, J. Qin, T. Racie, D. Raitcheva, K.G. Rajeev, D.W.Y. Sah, J. Soutschek, I. Toudjarska, H.P. Vornlocher, T.S. Zimmermann, R. Langer, D.G. Anderson, A combinatorial library of lipid-like materials for delivery of RNAi therapeutics, Nat. Biotechnol., 26 (2008) 561-569.
[33] V. Bitko, A. Musiyenko, O. Shulyayeva, S. Barik, Inhibition of respiratory viruses by nasally administered siRNA, Nat. Med., 11 (2005) 50-55.
[34] B.J. Li, Q.Q. Tang, D. Cheng, C. Qin, F.Y. Xie, Q. Wei, J. Xu, Y.J. Liu, B.J. Zheng, M.C. Woodle, N.S. Zhong, P.Y. Lu, Using siRNA in prophylactic and therapeutic regimens against SARS coronavirus in rhesus macaque, Nat. Med., 11 (2005) 944-951.
[35] Y.P. Zhang, W.B. Li, W.L. Wang, J. Liu, S.X. Song, L.L. Bai, Y.Y. Hu, Y.D. Yuan, M. Zhang, siRNA against plasminogen activator inhibitor-1 ameliorates bleomycin-induced lung fibrosis in rats, Acta Pharmacol. Sin., 33 (2012) 897-908.
[36] M.R. Zamora, M. Budev, M. Rolfe, J. Gottlieb, A. Humar, J. DeVincenzo, A. Vaishnaw, J. Cehelsky, G. Albert, S. Nochur, J.A. Gollob, A.R. Glanville, RNA Interference Therapy in Lung Transplant Patients Infected with Respiratory Syncytial Virus, Am. J. Respir. Crit. Care Med., 183 (2011) 531-538.
[37] E.J.B. Nielsen, J.M. Nielsen, D. Becker, A. Karlas, H. Prakash, S.Z. Glud, J. Merrison, F. Besenbacher, T.F. Meyer, J. Kjems, K.A. Howard, Pulmonary Gene Silencing in Transgenic EGFP Mice Using Aerosolised Chitosan/siRNA Nanoparticles, Pharm. Res., 27 (2010) 2520-2527.
[38] M. Kendall, S. Holgate, Health impact and toxicological effects of nanomaterials in the lung, Respirology, 17 (2012) 743-758.
[39] I. Bersani, S. Kunzmann, C.P. Speer, Immunomodulatory properties of surfactant preparations, Expert Rev. Anti-Infect. Ther., 11 (2013) 99-110.
[40] Y. Sun, Y.Q. Wang, R. Yang, J.J. Zhu, Y.Y. Le, J.G. Zhong, J. Lu, Exogenous porcine surfactants increase the infiltration of leukocytes in the lung of rats, Pulm. Pharmacol. Ther., 22 (2009) 253-259.